CRUSTAL PHASE PROPAGATION: DISCRIMINATION AND CORRECTIONS

G. Eli Baker, Mariana Eneva, Jeffry L. Stevens, and Heming Xu
Maxwell Technologies, Systems Division

Sponsored by the Defense Threat Reduction Agency
Contract No. DSWA-01-97-C0130

ABSTRACT

The primary objective of this work is to improve the accuracy of discrimination of nuclear explosions from earthquakes, by developing and implementing a transportable path correction algorithm for the Lg/Pg discriminant. A secondary result is the development of a depth discriminant based on Lg group velocity.

A key to understanding Lg and Pg amplitude changes, which can be dramatic over just 10s of kilometers, is using observations of such changes over short distances. We analyze changes in Lg and Pg along short paths between southern California seismic network (SCSN) stations for relationships between propagation and statistics of topography, gravity, and crustal thickness. A second key element of our approach is the use of categorical statistical techniques, which frees us from the common and generally unsupported assumption of a linear relationship between geophysical parameters and propagation. The principle underlying this approach is that distinct crustal or path types that have distinct effects on propagation can be characterized by geophysical parameters. The path types can include directionally dependent parameters. Corrections based on calibrated path types are then transported to uncalibrated areas with similar path types. This approach complements empirical methods that reduce the variance of existing data.

We use an inversion approach to extend the path correction techniques developed in southern California, to global data reported in the Reviewed Event Bulletins (REB), while maintaining the key elements of identifying path types and using short path segments. We divide long source-station paths into short segments, with each segment identified with a particular path type, and then invert for an Lg/Pg ratio correction factor for each path type. This performs comparably to other waveguide method approaches for single stations, but has the advantage of being applicable to multiple stations over a broad region.

Records with Lg or Pg below the background noise level contain important information regarding phase blockage. We use such censored data to determine path corrections and identify blockage. Estimation of Lg and Pg signal-to-noise (S/N) levels based on pre-event noise is common, but leads to inappropriate use of low S/N level measurements. The appropriate noise level to use is that of the pre-phase noise. Using the pre-event noise underestimates the real noise level for Lg and Pg, with the result that noise level measurements of those phases are used as if they were signal. We extend the inversion for path corrections to use low S/N measurements as upper bounds on the phase amplitudes in a Maximum Likelihood estimate, and apply it to the global data reported in the REB with the result that we clearly identify blockage.

We also test and model a depth discriminant based on Lg group velocity. We found in southern California, that Lg from earthquakes and explosions differ in their response to waveguide properties. This suggests that their Lg modal structures differ, which implies that Lg group velocities should differ for earthquakes and explosions. This is confirmed by observations from shallow and non-shallow sources in both SCSN and Israeli network data. The SCSN data consist of 582 high signal-to-noise (S/N) Lg recordings from 10 nuclear explosions, 3 non-shallow earthquakes, and one very shallow earthquake. The Israeli data consist of 630 recordings from 19 quarry blasts and 28 earthquakes, with near-surface to 22 km hypocentral depths. The depth dependent difference in Lg arrival times is significant and so provides a potentially useful depth discriminant. We use modal and finite difference synthetics to model the observations and gain further insight into their origin. Specifically, we examine the frequency-dependent effects on the arrival times of Lg of both modal excitation and Rg-to-Lg scattering in heterogeneous media.

OBJECTIVE

The primary objective of this research program is to improve the accuracy of discrimination of nuclear explosions from earthquakes by developing a transportable path correction algorithm for the Lg/Pg discriminant. A secondary result is the development of a depth discriminant based on Lg group velocity.

RESEARCH ACCOMPLISHED

Introduction

In this paper, we briefly review the development and application of path correction methods based on categorical techniques and southern California data. We focus on the underlying principles and basic results, and refer the reader to Baker and Eneva (1999) and Baker (1998) for details. We then describe the inversion approach used to generalize the method for use with long paths and apply it to data reported in the REB. We discuss the importance of recognizing low S/N data by using pre-phase rather than pre-event noise levels, and the incorporatation of censored data into the inversion. We demonstrate how use of low signal-to-noise level (S/N) measurements in a maximum likelihood estimate identifies Lg blockage, while inappropriate use of the measurements leads to spurious results, and we present results of inversions at a single station and over all of Asia. We conclude with a discussion of a depth discriminant based on Lg travel times. We present observations of late arriving Lg from shallow events in southern California and Israel, and mode and finite-difference modeling of the observations to assess different mechanisms.

Short paths between southern California stations, geophysical parameters, and statistical techniques

We compiled a data set of changes in Lg, Pg, and the Lg/Pg ratio between stations of the southern California seismic network (SCSN) together with statistics of topography, crustal thickness, and the isostatic gravity residual. Statistics used included the mean, median, maximum, minimum, roughness (various measures), average gradient, maximum slope, and second and third moments. Changes in absolute amplitudes of Lg and Pg were obtained by application of corrections for site amplifications, determined by Baker (1997). That permitted us to determine that changes in Lg are significantly larger and are more predictable than those in Pg (Baker, 1998).

We demonstrated (Baker, 1998; Baker and Eneva 1999) that assuming the relationship between propagation and various parameter values is linear will cause some such relationships to be missed altogether, while categorical techniques are appropriate to our assumption of the existence of distinct crustal types (or path types if we want to use directionally dependent parameters). We divided the path segments between stations into five types using cluster analysis and the statistics of parameters listed above, and found that analysis of variance soundly rejects the hypothesis that Lg propagation differences between the crustal types are due to chance (Baker, 1998). Even simple divisions of the crust into types by a single parameter, such as median elevation (in which case we define low, medium, and high elevation crust), is effective at reducing the variance in new data collected in the same area (Baker and Eneva, 1999).

We performed a test in which we clustered short paths between stations together with segments of longer paths between distant stations. We made corrections based solely on the short paths, and applied them to each segment of the long paths. This let us apply corrections based on calibrated areas (the short paths) to some areas without calibration data (some segments of the long paths) but with similar crustal types. The path corrections transported well from the southern Sierra to the Peninsula Range, and from other regions to the Salton Trough, reducing the scatter in the Lg/Pg ratio in both cases. On the other hand, corrections from the southwestern edge of the Mojave Block, when extended to the central and eastern Mojave Block, actually increased the Lg/Pg ratio scatter. In that case, the transport of corrections failed. The crustal types differ in their effects on propagation, but the geophysical parameters used did not distinguish between types. Paleomagnetic data indicates the far western Mojave Block has been strongly rotated relative to the eastern block (e.g. Dokka, 1997), and might have been useful in our study to further distinguish crustal types. This points out the need to thoroughly characterize areas in which corrections are to be extended.

An inversion extending use of short segments of distinct path types to long paths and global data

Previous work on waveguide method-based path corrections average parameters over entire paths (e.g. Rodgers et al., 1999; Lay et al, 1999). Average parameter values may however be misleading. For example, a path half in mountains and half in a basin may have the same average elevation as a path entirely within an high plateau, although the 3 crustal types mentioned likely affect propagation very differently. Thus it is improtant that we continue to base corrections on short path segments. Previous work also has focused on corrections at single stations. For corrections to have a plausible physical basis, they must provide the same correction value for similar paths, even to different stations. To retain the use of short path segments and enable corrections to be made over an entire region utilizing multiple stations, we perform an inversion for correction terms for each crustal type based on the equation $a_i = \sum c_k \bullet d_k$, where a_i is the i^{th} $\log_{10}(Lg/Pg)$ ratio, c_k is the correction term for the k^{th} crustal type, and d_k is the distance of the k^{th} crustal type that makes up the i^{th} event-station path. This can be written in matrix form as

$$\begin{vmatrix} d_{11} & d_{12} & \dots & d_{1n} \\ d_{21} & d_{22} & \dots & d_{2n} \\ . & & & . \\ . & & \dots & . \\ d_{m1} & d_{m2} & \dots & d_{mn} \end{vmatrix} \bullet \begin{vmatrix} c_1 \\ c_2 \\ . \\ . \\ c_n \end{vmatrix} = \begin{vmatrix} a_1 \\ a_2 \\ . \\ . \\ . \\ a_m \end{vmatrix} \qquad (1)$$

and when there are no censored data, can solved as a simple least squares problem. We present an example of this next.

Figure 1 shows the event-station paths from the June 1996 through October 1999 REB, having S/N > 2 for both Lg and Pg. For this very simple test, we divide the crust into types based on increments of sediment thickness (<50 m, 50-200 m, 200-500 m, 500-750 m, 750 m-1 km, 1-2 km, 2-4 km, 4-6 km, 6-8 km, 8-10 km, and > 10 km). Most of the paths cross areas with less than 2 km of sediments, and there are virtually no paths that cross sediments thicker than 6 km. so we effectively fit 8 parameters to 414 Lg/Pg ratios.

In addition to the distance correction, we achieve an 11% σ^2 reduction, and a 24% $SMAD^2$ reduction (the scaled median absolute deviation, SMAD, is the one-norm equivalent of the standard deviation and is a more appropriate measure of scatter for these clearly non-Gaussian distributions). This demonstrates that a small set of correction terms can reduce the Lg/Pg scatter at many stations over a large region.

Recognizing and using censored data to refine path corrections and identify blockage

When a phase is blocked, the measured phase amplitude will be below the pre-phase noise level. Such records are the most important to identifying blockage. When we have such data, the amplitude measured in the phase window is used as an upper bound on the true phase amplitude. Because we use amplitude ratios, we have doubly censored data. When data are censored, we use maximum likelihood estimation to solve equation 1. We present two examples in which this approach identifies areas of blockage. In the first, we use data at a single station to demonstrate the errors that occur when such censoring is not recognized and dealt with appropriately. In the second, we demonstrate the capability of this approach to automatically identify areas of blockage using multiple stations over a larger area.

There are two important issues regarding censored data. The straightforward one is how to analyze it. Bias due to censored data has long been recognized in seismic magnitude estimation (e.g. Ringdal, 1977), and methods of incorporating such data into an inversion are well understood. The more subtle issue for path correction studies appears to be recognizing that data are censored. A surprising and ubiquitous error made in this sort of study is that S/N levels used to select "good" data are determined by comparing amplitudes within Lg and/or Pg signal windows with pre-event noise levels (e.g. Xie and Mitchell, 1990; Lay et al, 1999; Rogers et al, 1999). This is an error. For phase measurements to be plausibly recognized, they must have greater amplitude than the coda of preceding phases. Ignoring this can have serious ramifications, as

the "Lg" measured, for example, may actually represent the amplitude of Pn, Pg, or Sn coda. This undermines the basis for any physical interpretations of results that may be obtained.

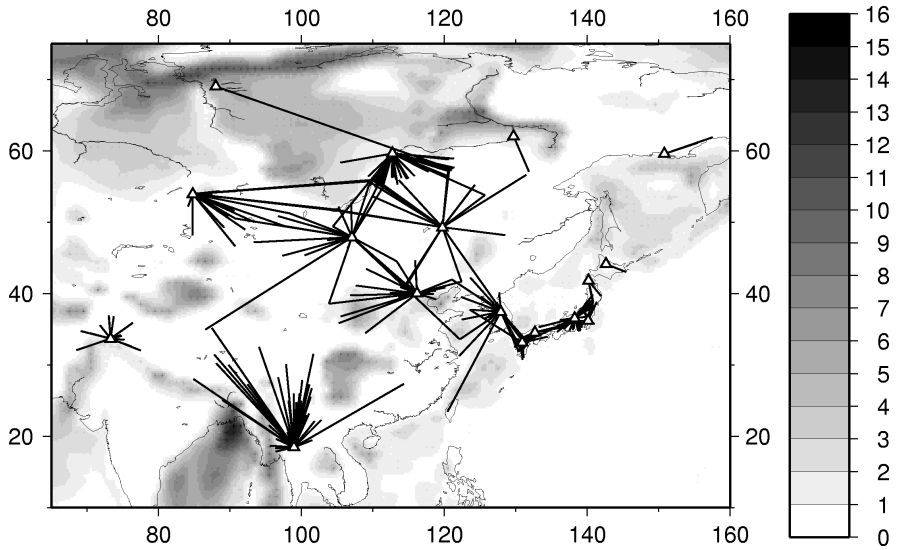

Figure 1: Event-station paths (triangles denote stations) for events with both Lg and Pg S/N > 2 as reported in the June 1996 to Oct. 1999 REB, overlain on a sediment thickness contour map (contour scale is in km).

In the next simple example, we will temporarily neglect the issue of transportability in order to make a single point clearly. That is, we address the effect of using noise level measurements as if they are signal and show how appropriate incorporation of noise level measurements can be used to identify blockage. Thus, although we use the method of dividing the crust into types, we do so very simplistically for just a single station and want to make it clear that we do not suggest that all low elevation crust will block Lg. It is just coincidental that for the paths to this one station, the areas that block Lg are low elevation.

A typical example of waveguide-based path corrections, using data from ZAL, was reported by Lay et al (1999), so we perform a similar analysis using our inverse approach, this time separating crustal types by elevation. We perform the analysis two ways. First, we purposely make the mistake described above. That is, we compare signal amplitudes to pre-event rather than pre-phase noise levels, so that noise level measurements may be used as if they are signal amplitudes. Then we repeat the analysis, but with poor S/N records properly identified as noise level measurements.

From June 1996 through October 1999, the REB reported 433 events with Pn S/N > 2. Of those, only 65 had Lg signal greater than pre-Lg noise. Thus, in our first inversion 85% of the data input as Lg signal measurements really repesent coda amplitudes of earlier phases. The corrections therefore are really due to fitting parameters to the ratio of Pn to Pn, Pg, and/or Sn coda. Both Lay at al (1999) and our first inversion produced an approximately 40% variance reduction due to the distance correction, but only a few percent more for the waveguide based corrections. Figure 2 demonstrates why that is the case. In the top plot, $\log_{10}$(Pn/Lg) is binned for all the data regardless of Lg S/N level, and plotted versus distance (each plot uses 22 points/bin). The large variance reduction with distance is due to the strong relationship demonstrated by this plot. The data however more likely represents the ratio of Pn to Pn coda, rather than Pn to Lg amplitude. The middle plot shows $\log_{10}$(Pn/Lg) of all 433 data points again, plotted vs. mean elevation. There is no apparent relationship, which explains why the waveguide-based corrections provided little further variance reduction. In the bottom plot, we have separated the data into two groups. Recall that all the data have Pn S/N > 2, but now one data set (the upper curve) contains the 368 data points with Lg S/N < 2 (where the noise is pre-Lg noise). For that data set there is still no relationship between mean elevation and relative propagation efficiency. The lower curve is from the 65 data points with Lg S/N > 2. That curve does show a clear relationship between elevation and relative propagation efficiency. The

overall Pn/Lg ratio is of course much smaller, as the noise amplitudes erroneously used as Lg signal amplitude are much larger than the real signal amplitudes. Inversion results are presented in Table 1.

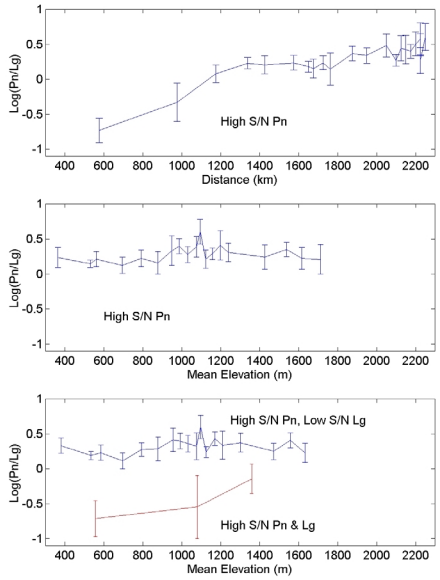

Figure 2: Log_{10}(Pn/Lg) vs. distance (top) and log_{10}(Pn/Lg) vs. mean elevation along the event-station path (middle), both for all data regardless of Lg S/N level In these two cases Lg amplitude may actually reflect amplitude of earlier phase coda. The bottom plot is log_{10}(Pn/Lg) for low S/N Lg (upper curve) and for high S/N Lg (lower curve). All data are binned with 22 data points/bin. The median and two SMAD deviation confidence intervals are plotted.

Crustal Type by Elevation	Noise as Signal	High S/N Only	Censored Data
-.2-.3 km	0.5170	0	-19.9664
.3-.8 km	0.2102	0.025	0.1099
.8-2 km	-0.1165	-0.586	-0.3616
2-3 km	-0.1380	0.224	0.9591
3-4 km	0.6908	0.329	-0.0968
>4 km	0.2481	1.135	0.5170

Table 1: Results of two inversions for path corrections to ZAL. In both, we divide the crust into 6 types based on elevation. As described above (equation 1), we determine the distance each path traverses each crustal type. The important result in this example is the correction term for the lowest elevation crustal type, -200 to 300 meters (top row).

In the 1st inversion, we use Lg noise levels as if they are signal (second column). In that case the large number, relative to other correction terms, (top row) erroneously predicts a small Pn/Lg ratio. In the 2nd inversion, we appropriately use Lg noise levels as upper bounds on signal amplitudes in a maximum likelihood estimate. As an intermediate step, we determine the least squares solution to equation 1 for just the high S/N data. There, the correction term for the lowest elevation group is zero (3rd column), since no paths with good Lg S/N traverse such paths. Finally, when we incorporate the censored data into a maximum likelihood estimate (last column), the correction term for the lowest elevation group is a huge negative number, correctly identifying that crustal type as blocking Lg.

We are not saying that all low elevation paths to all stations, block Lg. Only in this example using data recorded at ZAL to demonstrate the importance of recognizing and appropriately using censored data, do all the low elevation paths happen to block Lg.

The purpose of this final example is to demonstrate that censored data can be used to systematically identify blockage within a large region using multiple stations. To do so, we use a much simpler approach than identifying crustal types. We invert for blockage and relative Pn to Lg attenuation just for latitude-longitude grids. Thus, for this example we are not addressing transportability. This demonstration that maximum likelihood estimation using censored data can identify blockage over a large region sets the stage for future work, which should use more well-defined path types as inversion parameters. For this example, our inversion parameters are simply geographic grid locations, and the data are Lg/Pn amplitude ratios reported in the REB for all the Asian stations from June 1996 through October 1999. We select only data where the paths do not cross oceanic crust. For reasons we do not understand, the REB report a large number of high S/N Lg measurements from event-station paths crossing deep ocean. We do not address this problem here, but remove such data from our inversion data set. This leaves us 1834 measurements. Low S/N level phase amplitudes are treated as upper bounds on the amplitudes. We invert for path effects for all 3°x3° geographic grids that had at least 40 1° long path segments pass through them. Figure 3 shows that

two areas of blockage are identified (darkest tiles). The most northeastern dark area covers a transition from no sediment cover to the east, to a thick (7 km) sedimentary basin to the west. The westernmost dark area corresponds to another thick (7.65 km) sedimentary basin. Thus, despite the coarse spatial averaging of this simple example, two major areas of blockage were automatically identified.

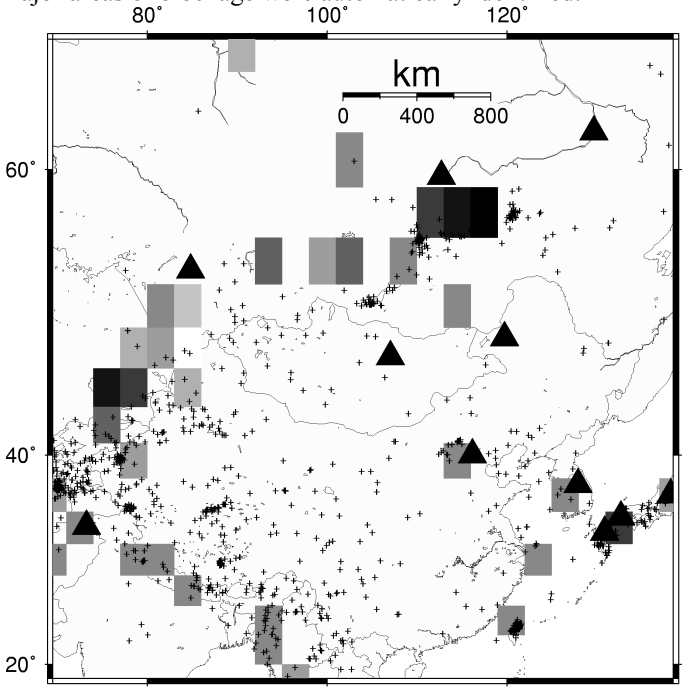

Figure 3: 3x3 degree grids through which passed at least 40, one degree long path segments, along with the locations of 1317 events (dots) and 18 stations (triangles) used in the inversion The important result is that the darkest grid cells were found to block Lg.

Lg arrival times: a resurrected depth discriminant

We noted earlier that Lg propagation effects related to waveguide properties differ in southern California, depending on whether the source is an earthquake or explosion. The simplest explanation for this is that the shallower sources preferentially excite shallowly propagating modes, relative to the deeper sources. If so, we should observe a difference in Lg arrival times. It has long been recognized that Lg arrivals from shallow sources can be delayed relative to Lg from deeper sources. Pomeroy, et al. (1982), for example, listed this depth dependence among possible regional earthquake/explosion discriminants, but abandoned the idea because of the inconsistency of the observations. The data however were analog and typically around 1 Hz or below. We find that the discriminant is much more likely to be successful today with greater bandwidth and digital data permitting better waveform processing techniques. Figure 4 shows two waveforms at 369 km from an earthquake and 340 km from an underground nuclear test at the Nevada Test Site recorded at the same station. The time window defined by group velocities of 3.6 to 3.0 km/second is marked on each record. Notice how much later in the window the Lg arrival from the explosion occurs compared to the arrival of the deeper earthquake.

Figure 4 also illustrates the method used to measure Lg arrival times. Unlike other seismic phases, Lg is not associated with displacements propagating along a well-defined ray path and so there is no distinct model dependent travel-time for the phase and no travel-time residual. Rather, Lg is defined as whatever energy arrives within a particular group velocity window, usually around 3.6 to 3.0 km/sec, and is modeled either as shear waves trapped in the crustal waveguide or as higher mode surface waves. To quantify the relative delay between seismograms, we use the median cumulative amplitude (MCA) of the envelope function of Lg (Figure 4). That is, the MCA is the position that evenly divides the area under the curve of the envelope function into two halves. Because the length of the Lg group velocity window changes with distance, the midpoint is normalized by the window length and is expressed as a fraction of total window length.

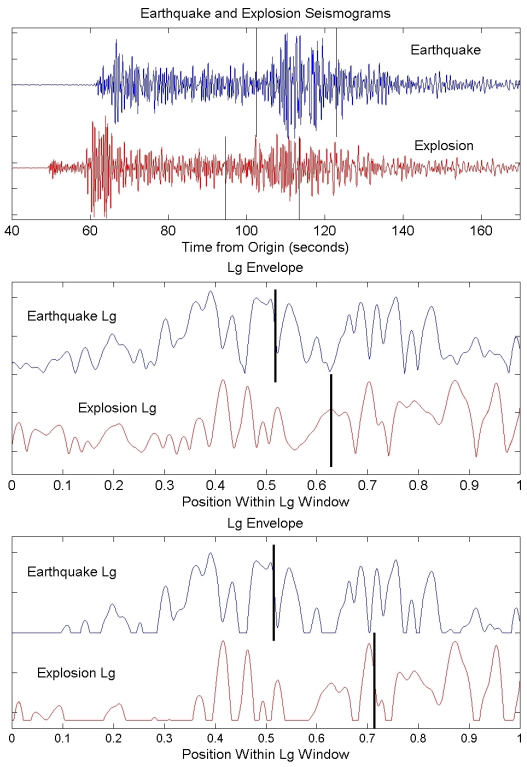

Figure 4. Seismograms (upper plot) from an earthquake at 369 km distance (upper trace) and a nuclear explosion at 340 km distance (lower trace), both recorded at the same station, with the position of the Lg windows bracketed by vertical lines. The envelope functions of just the Lg windows are plotted versus position within the Lg window (middle plot), with the median cumulative amplitude (MCA) positions indicated by vertical lines. Better separation of shallow events occurs when the MCA is determined from only those values of the Lg envelope greater than the mean value of the pre-Lg noise window envelope function (pre-Lg window not shown). The lower plot shows the Lg envelope functions with that correction, and their MCAs (vertical lines).

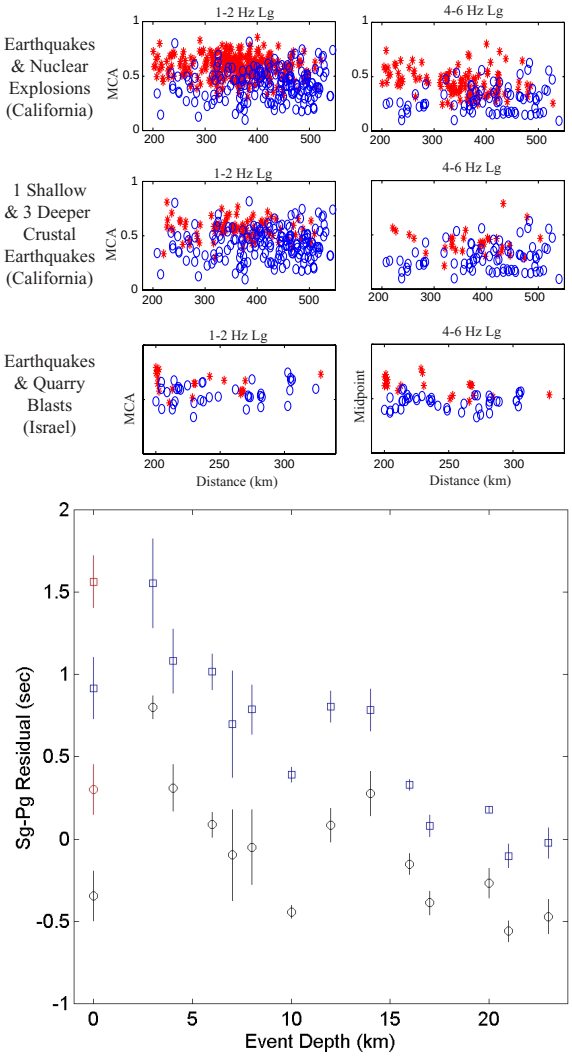

Figure 5. The upper plot shows 3 examples in 2 passbands in which a measure of Lg arrival times (described in Figure 4) is plotted for shallow events (asterisks) and non-shallow earthquakes (circles), vs. distance. The shallow event Lg is always later. The lower plot shows Sg minus Pg residual travel times vs. source depth for 133 local (< 75 km distance) Israeli earthquakes and 33 quarry blasts. The median earthquake Sg minus Pg residuals dencrease with depth throughout the entire seismogenic crust, relative to both IASPEI91 (used by the IMS, squares) and the Israeli velocity model (circles). Quarry blast Sg minus Pg residuals relative to each model are also shown (red, at z=0). This clearly shows that shear wave arrival times depend strongly on source depth throughout the crust. That is, the differences observed at top are not just a near surface effect, but rather, each increment of source depth affects the shear wave travel time

Figure 5 presents observations that demonstrate the effect of depth on S phase arrival times. We found that in all cases - Lg from a very shallow earthquake (1-2 km source depth) vs. non-shallow earthquakes recorded at the SCSN, Lg from NTS nuclear explosions vs. non-shallow earthquakes recorded at the SCSN, and Lg from quarry blasts vs. from 6-22 earthquakes recorded in Israel - the shallow event Lg was slower. No differences were observed in Pg travel times. In addition, for near source observations in Israel, earthquake Sg was delayed relative to Pg as a function of depth from 0 to 22 km deep sources.

Mode synthetic seismograms for sources from 1 to 30 km depth, in 1 km intervals, are shown in Figure 6. There is clearly more energy later in the Lg window of the shallow event seismograms. This observation is quantified in Figure 7, where the MCAs of the Lg windows of the synthetics' envelope functions are plotted vs. source depth. There is also considerably more energy in shallowly propagating modes with lower group velocities than those that bracket the Lg window. In the real Earth, scattering at the surface and by velocity heterogeneities may scatter some of that energy into higher velocity modes. That is essentially the mechanism commonly proposed for the enhancement of Lg by the fundamental mode (e.g. Myers et al, 1999). We examine that mechanism next using finite-difference synthetics.

We use finite-difference modeling to examine the effects of scattering on Lg. This demonstrates how energy may be scattered from Rg to Lg, causing the observed delays of Lg for shallow events. We calculate synthetics for a range of earthquake depths and distances, for both the model of Figure 6 and that same model with random heterogeneities added. The heterogeneities are zero mean Gaussian, with a correlation length of 2.25 km. and a standard deviation of 10% of the velocity in the surface layer, dropping to 7% in the lower crust. The Poisson ratio remains the same as in each layer of the homogeneous model.

Figure 8 shows synthetic seismograms for the homogeneous and heterogeneous models, for earthquakes at 1 km. depth intervals from the surface to the Moho, at 30 km. The Lg window, from 3.6 to 3.0 km/sec group velocity, is outlined by shadowing. The homogeneous model synthetics (left) look much like the mode synthetics, but in this case the fundamental mode is included (labeled Rg). The seismograms are similar those in Figure 6 (the mode synthetics), but have more detail, as the solution is more complete than that of the mode summation. Rg is only generated by very shallow sources and is much larger in the homogeneous model case, as are the higher modes, than for the heterogeneous model (right). Seismograms from propagation through the heterogeneous model have the energy distributed more evenly throughout the record. These simulations demonstrate that Rg to Lg scattering may also be a feasible mechanism for delaying Lg arrivals.

Further observations and modeling support the modal explanation for late arriving Lg from shallow events. In particular, we observe better event separation at higher frequency. This is predicted by the modal explanation, as the modes are more narrowly constrained in depth at higher frequency. The Rg to Lg scattering model however, would predict later Lg at lower frequency, since the higher frequency Rg scatters out away much more rapidly. Near source observations of Israeli quarry blast records confirm this. Below 1 Hz, Rg persists up to 100 km distance from sources and records tend to have energy in either Rg or Lg, but not in both. The mutual exclusivity of Rg and Lg suggests that below 1 Hz, Rg may be a major contributor to Lg. At higher frequencies however, where depth discrimination is stronger, there is no clear Rg beyond 20 km, and no apparent mutual exclusivity between Rg and Lg.

CONCLUSIONS AND RECOMMENDATIONS

Studies using the closely spaced SCSN data identified two factors important to successful transport of waveguide method-based path corrections for Lg to P discriminant values. One is that parameters should not be averaged over entire paths, but rather, long event-station paths should be broken up into small segments. The second is that the assumption of linear relationships between propagation effects and parameter values can miss important relationships, whereas categorical statistics techniques allow us to model propagation based on the assumption that distinct crustal types exist and affect propagation differently from each other. These crustal types can be generalized to path types, so that directional parameters, such as whether the crust in thinning or thickening in the ray direction, can be incorporated.

An inverse method was developed to retain these key elements while determining path corrections for the long event-station paths reported in the REB. It was shown to be effective in an application to all the Asian data reported over 3 years. The method reduces the Lg/Pg scatter for the region using just 8 parameters based on sediment thickness. More refined path type separation, such as the cluster analyses performed for SCSN paths, should be performed. We expect that would provide even greater reductions in scatter.

In the area of path corrections, we recommend for all REB data, that path types be clustered based on statistics of all possible geophysical parameters and censored data be identified and incorporated into the maximum likelihood inversion described here. This will result in a valid map of phase blockage most relevant to IMS stations. This should be performed for as narrow of depth range sources as possible, and refined as more accurate depths and more ground truth data become available. For the path corrections, rigorous error analyses must be performed to assess the accuracy of transportability.

We have made observations of delays in Lg and Sg from shallow events relative to non-shallow events in 2 regions of the world. The delays are large and consistent enough to discriminate depth, with better discrimination at higher frequency. Modeling indicates that the delay is due to excitement of different modes by different depth sources. We recommend that an Lg group velocity discriminant be regionalized for all IMS stations. An effective depth discriminant will depend on accurate regionalized travel time models, and the regionalized discriminant must be rigorously tested using all available ground truth data.

Lg being composed of different modes has profound implications for CTBT monitoring. Path corrections for discriminants, as well as travel times, may not be valid for events at depths other than those of the calibration events. Ensuring the validity of any type of Lg correction surface will depend on our understanding of the source depth effect on Lg and our ability to more accurately assess source depth.

Determination of whether a measurement represents a signal or noise level must be made using pre-phase, not pre-event, noise levels. We have demonstrated that once this is done, noise level measurements incorporated into a maximum likelihood estimate can automatically and accurately identify areas of blockage. We have also demonstrated how the inappropriate use of noise levels as if they are signal amplitudes, a common error, can easily lead to erroneous conclusions.

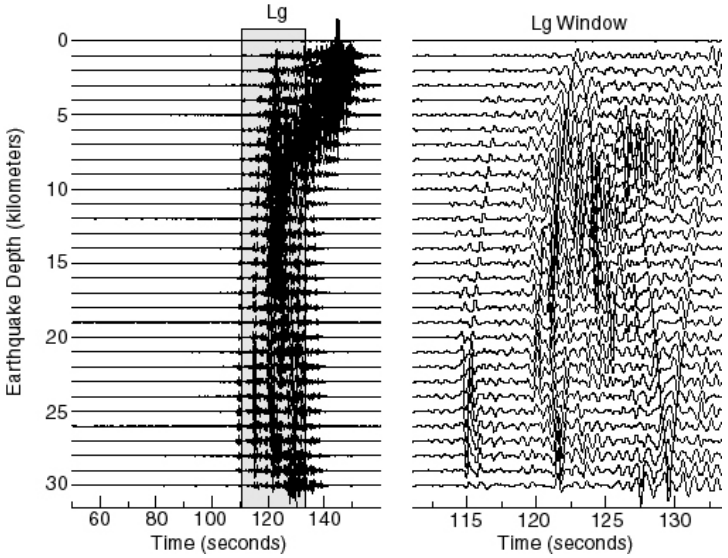

Figure 6: Mode synthetics (sans fundamental mode) at 400 km distance, for a model from the NTS to southern California region (Asad, 1998) and for 0 to 30 km depth sources. Modes excited in shallow layers are larger for shallow sources and so make a greater contribution to later Lg. The left plot shows seismograms from 8.0 to 2.5 km/sec group velocities. The Lg window is shaded. On the right is just the Lg window, from 3.6 to 3.0 km/sec group velocity.

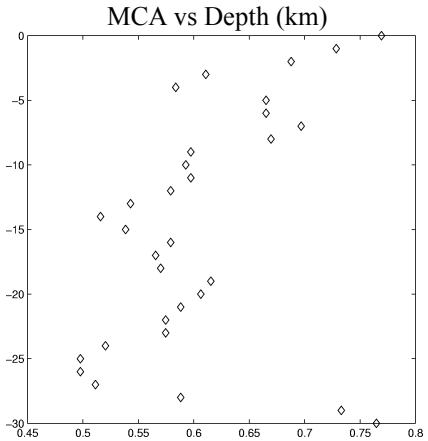

Figure 7: Median cumulative amplitude (MCA) positions of Lg envelope functions, for the seismograms shown in Figure 6). Excitation of different modes is consistent with observed delays of shallow-event Lg.

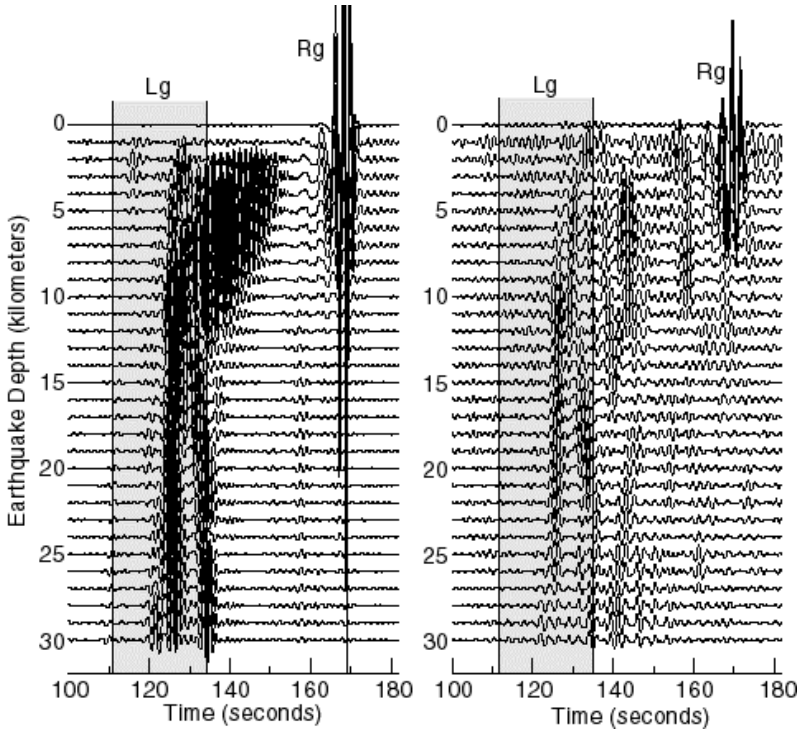

Figure 8: Seismograms at 400 km distance for the homogeneous model (left), and for sources from 0 to 30 km depth, from 4.0 to 2.2 km/sec group velocity, with the Lg window (3.6 to 3.0 km/sec group velocity) indicated by shadowing. The very large Rg for shallow events in the homogeneous model is purposely clipped, to allow more details of the smaller phases to be seen. The right plot shows the same for the heterogeneous model. All traces are plotted on the same scale.

Key Words: discrimination, event depth, blockage, Lg, path correction, propagation

REFERENCES

Asad, Abu Muhammad (1998), Linearized and nonlinear travel time tomography for upper crustal velocity structure of the western Great Basin, Ph.D dissertation, University of Nevada, Reno

Baker, G.E., 1998, Predicting crustal phase propagation efficiency from topography, gravity, and crustal thickness, *Proc. 20th Annl. Seism. Res. Symposium on Monitoring a CTBT*, pp. 153-162

Baker, G.E. and M. Eneva, 1999, Predicting Crustal Phase Propagation from Other Geophysical Parameters, *Proc. 21st Annl. Seism. Res. Symposium on Monitoring a CTBT*, pp. 7-17

Dokka, R. K., 1997, Multiple, large early Miocene vertical axis rotations in the west-central Mojave Desert and implications for the tectonic development of southwestern Cordillera, *GSA Abs. w. Progs,* **29**, p. 279

Lay, T., G. Fan, R.S. Wu, and X.B. Xie, 1999, Path corrections for regional phase discriminants, *Proc. 21st Annl. Seism. Res. Symposium on Monitoring a CTBT*, pp 510-519

Myers, S., W. Walter, K. Mayeda, and L. Glenn, 1999, Observations in support of Rg scattering as a source of explosion S waves: regional and local recordings of the 1997 Kazakhstan depth of burial experiment, *BSSA*, pp. 544-549

Ringdal, F., 1977, Maximum likelihood estimation of seismic event magnitude, *BSSA*, **67**, pp. 789-802

Rodgers, A., W. Walter, C. Schultz, S. Myers, L. Thorne, 1999, A Comparison of Methodologies for Representing Path Effects on Regional P/S Discriminants, *BSSA*, **89**, pp. 394-408

Xie, J. and B.J. Mitchell, 1990, A back projection method for imaging large scale lateral variations in Lg coda Q with application to continental Africa, *Geophys. J.*, **100**, 161-181